Discovery of STRO-002, a Novel Homogeneous ADC Targeting Folate Receptor Alpha, for the Treatment of Ovarian and Endometrial Cancers

Xiaofan Li[1], Sihong Zhou[1], Cristina L. Abrahams[2], Stellanie Krimm[3], Jennifer Smith[1], Krishna Bajjuri[1], Heather T. Stephenson[4], Robert Henningsen[1], Jeffrey Hanson[1], Tyler H. Heibeck[1], Daniel Calarese[1], Cuong Tran[1], Gang Yin[1], Ryan L. Stafford[5], Alice Y. Yam[1], Toni Kline[6], Venita I. De Almeida[7], Aaron K. Sato[5], Mark LupherJr, Kristin Bedard[1], and Trevor J. Hallam[1]

ABSTRACT

STRO-002 is a novel homogeneous folate receptor alpha (FolRα) targeting antibody–drug conjugate (ADC) currently being investigated in the clinic as a treatment for ovarian and endometrial cancers. Here, we describe the discovery, optimization, and antitumor properties of STRO-002. STRO-002 was generated by conjugation of a novel cleavable 3-aminophenyl hemiasterlin linker-warhead (SC239) to the nonnatural amino acid *para*-azidomethyl-L-phenylalanine incorporated at specific positions within a high affinity anti-FolRα antibody using Sutro's XpressCF+, which resulted in a homogeneous ADC with a drug–antibody ratio (DAR) of 4. STRO-002 binds to FolRα with high affinity, internalizes rapidly into target positive cells, and releases the tubulin-targeting cytotoxin 3-aminophenyl hemiasterlin (SC209). SC209 has reduced potential for drug efflux via P-glycoprotein 1 drug pump compared with other tubulin-targeting payloads. While STRO-002 lacks nonspecific cytotoxicity toward FolRα-negative cell lines, bystander killing of target negative cells was observed when cocultured with target positive cells. STRO-002 is stable in circulation with no change in DAR for up to 21 days and has a half-life of 6.4 days in mice. A single dose of STRO-002 induced significant tumor growth inhibition in FolRα-expressing xenograft models and patient-derived xenograft models. In addition, combination treatment with carboplatin or Avastin further increased STRO-002 efficacy in xenograft models. The potent and specific preclinical efficacy of STRO-002 supports clinical development of STRO-002 for treating patients with FolRα-expressing cancers, including ovarian, endometrial, and non–small cell lung cancer. Phase I dose escalation for STRO-002 is in progress in ovarian cancer and endometrial cancer patients (NCT03748186 and NCT05200364).

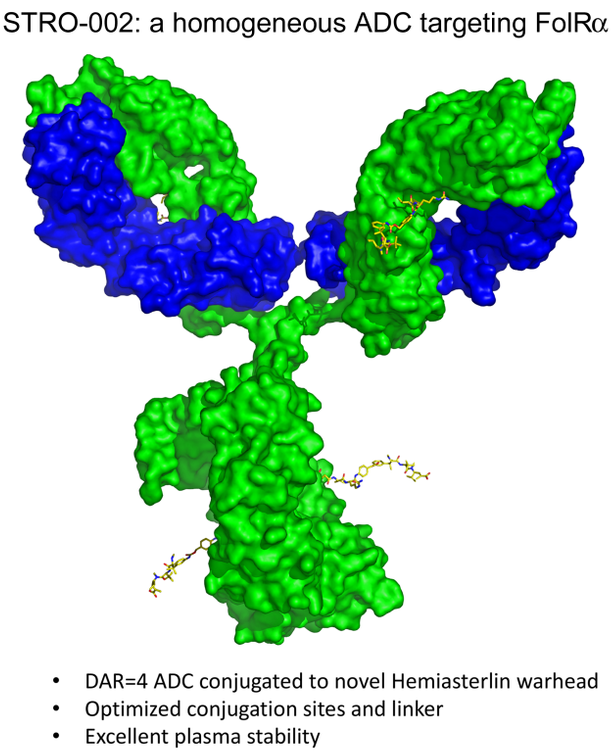

Introduction

In the United States, gynecologic cancers account for more than 10% of all cancers in women and are known for their aggressive nature at advanced stages (1). Ovarian cancers are often asymptomatic at early stages, resulting in late-stage diagnosis and poor prognosis with a 5-year survival rate of only 49.1% (2). Endometrial cancer is the most common gynecologic cancer in the US and is the only gynecologic cancer that has increased both in incidence and mortality in recent years (3). Despite the recent progress in targeted therapies and immunotherapies, surgical removal and chemotherapy remain the standard of care (SOC) for patients with ovarian and endometrial cancer (2, 4) and there persists to be an unmet medical need for treatments in metastatic, recurrent, and chemotherapy-resistant diseases.

[1]Sutro Biopharma, South San Francisco, California. [2]Seagen, South San Francisco, California. [3]Genentech, South San Francisco, California. [4]Gilead, Foster City, California. [5]Twist Bioscience, South San Francisco, California. [6]Engine Biosciences, San Carlos, California. [7]3T Biosciences, South San Francisco, California.

Corresponding Author: Xiaofan Li, Sutro Biopharma, 111 Oyster Point Blvd, South San Francisco, CA 94080. Phone: 650-801-6434; E-mail: xli@sutrobio.com

Mol Cancer Ther 2023;22:155–67

doi: 10.1158/1535-7163.MCT-22-0322

Folate receptor alpha (FolRα), a glycosylphosphatidylinositol (GPI)-linked cell-surface glycoprotein, binds and internalizes folic acid to support DNA and RNA synthesis during cell proliferation (5). While FolRα is normally expressed at low levels on the luminal surface of a small number of organs, high levels of FolRα have been observed in several malignancies, such as ovarian cancer, endometrial cancer, non–small cell lung cancer (NSCLC), and triple-negative breast cancer (TNBC; ref. 5). Overexpression of FolRα on solid tumors may regulate cell growth and signal transductions that leads to a growth advantage for cancer cells (6). Importantly, FolRα expression is persistent in metastatic or recurrent tumors and after chemotherapy (7), which makes FolRα a clinically relevant target for treatment of ovarian and endometrial cancers.

Antibody–drug conjugates (ADC) are a rapidly growing class of targeted therapeutics that combine the favorable pharmacokinetics profile and tumor targeting properties of antibodies with the potent cell killing activity of an attached warhead, which results in a more precise delivery of cytotoxic drugs to the tumor (8). To date, 12 ADCs have been approved by the FDA, and more than 100 ADCs are at different phases of clinical development across a range of indications (9). While early efforts to target FolRα using a monoclonal antibody (farletuzumab, MORAb-003, in combination with carboplatin and taxane) did not meet the study's primary end point (10), mirvetuximab soravtansine (IMGN853), an anti-FolRα ADC, improved clinical objective response rates to 24% in high FolRα expressing tumors compared with chemotherapy (10%) in a Phase III trial for patients with ovarian cancer (11). A second FolRα-targeting ADC, MORAb-202, is currently in Phase I/II trials for multiple solid tumor indications including ovarian and endometrial cancers (12).

Here, we describe the preclinical development of STRO-002, a homogeneous FolRα targeting ADC with a drug–antibody ratio (DAR) of 4. STRO-002 was produced using Sutro's protein expression platform XpressCF+ and copper-free click chemistry, which enabled the rapid optimization of an anti-FolRα ADC with favorable stability, *in vitro* cytotoxicity, and *in vivo* antitumor efficacy. STRO-002 displays potent specific cytotoxicity toward FolRα-expressing tumor cells and bystander killing of FolRα-negative cells when cocultured with FolRα-positive cells. With superior stability and a favorable pharmacokinetics (PK) profile in mice, we have further demonstrated statistically significant suppression of ovarian and endometrial cancer models *in vivo* in response to STRO-002 monotherapy or in combination with approved SOC agents. Phase I dose escalation for STRO-002 is in progress in ovarian cancer and endometrial cancer patients (NCT03748186 and NCT05200364).

Materials and Methods

Cell lines

KB, OVCAR3, OV90, A549, SKBR3, MDA-MB-453, MDA-MB-231, MDA-MB-468, HCT116, HT29, Skco1, NCI-H1703, A549, NCI-H1651, NCI-H2110, NCI-N87, A431, SU-DHL-6, Daudi, MES-SA, and MES-SA/MX2 cells were purchased from ATCC. OPM2 cells were purchased from The Leibniz Institute DSMZ (German Collection of Microorganisms and Cell Cultures GmbH). OVKATE and OVSAHO cells were purchased from Sekisui Xeno Tech. Igrov1 cells were licensed from NCI. Short tandem repeat profiling was conducted for all cell lines to ensure authenticity.

Generation and analysis of STRO-002

The anti-FolRα Ab SP8166 was discovered by ribosome display and the final sequences were listed in patent WO2019055931A1 (13) as HC variable domain (sequence#362), HC constant domain (sequence#370), LC variable domain (sequence#367), LC constant domain (sequence#371). SP8166 was expressed in Xpress+ CF with *para*-azidomethyl-L-phenylalanine (pAMF) incorporated at HC-Y180 and HC-F404 sites using a process previously described (14).

Cell-free reactions are performed at 25°C for 14 hours. Antibody was captured on MabSelect Sure (GE Healthcare), eluted in 50 mmol/L Sodium Acetate pH 3.3, and neutralized to pH 7 with 1 mol/L Tris Base, polished by preparative SEC (Superdex 200 Increase 10/300 GL) and equilibrated in 1xPBS. For the generation of SC239 conjugates, SC239 in DMSO was incubated with SP8166 (1 mg/mL) at a SC239 to pAMF ratio of 3 in PBS with 25% of DMSO at room temperature overnight. Excess free drug was removed by cation exchange. The conjugates were formulated in 10 mmol/L citric acid, pH 6 with 9% sucrose, sterilized through a 0.22-μm filter, and stored at 4°C. The conjugation was verified by LC/MS and DAR was calculated using the method below.

DAR determined by LC/MS

ADCs were separated using an Agilent PLRP-S HPLC column (2.1×50 mm, 1,000Å, 5 μmol/L). The mass data was acquired on an Agilent 6520A Accurate Mass Q-TOF MS. All spectra were extracted using MassHunter Qualitative (B6.00) from Agilent. The DAR value was calculated using DAR Calculator B.1.0 (Agilent Technologies).

SPR kinetic analysis

Kinetic analysis was performed using a Biacore T200 (GE Life Sciences). Anti-human Fc polyclonal antibodies (Jackson ImmunoResearch) were immobilized onto a CM4 chip (GE Life Sciences) using Amine Coupling Kit (GE Life Sciences). SP8166 was then captured on the anti-Fc surface. Recombinantly-expressed FolRα extracellular domain (ECD; Acro Biosystems) at concentrations from 0 to 300 nmol/L was allowed to associate to SP8166 for 540 seconds followed by a 600-second dissociation phase. Data analysis was performed using Biacore T200 Evaluation software. The raw data was double reference subtracted and binding curves in the appropriate range were globally fit with a 1–1 Langmuir binding model with constant RI of 0. Binding affinity (KD, M) was determined as a ratio of the kinetic rate constants (kd/ka, M) calculated from the fits of the association and dissociation phases.

FACS-based cell binding assay

Cells were harvested using Accutase (Innovative Cell Technologies), counted by the Vi-CELL Cell Viability Analyzers (Beckman Coulter) and resuspended in FACS buffer (PBS buffer supplemented with 1% BSA, 0.05% sodium azide). Cells were incubated on ice with serial dilutions of anti-FolRα antibody for 60 minutes. After washes with ice-cold FACS buffer, the cells were incubated with Alexa 647 labeled donkey anti-human Fc antibody (Jackson ImmunoResearch) on ice for another 60 minutes. Samples were analyzed using a BD FACS Canto system and geometric mean fluorescence intensities were fitted using with one site-specific binding equation on GraphPad Prism.

STRO-002 internalization assay

FolRα-positive Igrov1 and OVCAR3 cells were incubated with SP8166-Alexa647 at a saturating concentration (100 nmol/L) on ice for 1 hour. After three washes, internalization was initiated by adding 300 μL warm (37°C) cell culture medium to the cells. The plates were then covered and incubated at 37°C in a CO_2 incubator. At different time points after incubation, two plates were taken out and the cells were spun down at 4°C. One plate was kept on ice and used as an

"unquenched" sample. For the other plate, 200 μL/well of ice-cold quenching buffer (PBS, pH = 3 adjusted by HCl) was added to remove the non-internalized antibodies ("quenched" samples). After washes, the unquenched and quenched samples were analyzed using BD FACS Canto. Percentage of internalization was calculated as (quenched MFI)/(unquenched MFI). Quenched samples at different time points were also observed under a fluorescent microscope (EVOS M5000, Thermo Fisher) to monitor the internalization process.

Free drug– and ADC-mediated cytotoxicity assay

For 2D cytotoxicity assay, cells were plated on TC coated 96-well cell culture plate the day before the assay and treated with a serial dilution of ADC or free drug for 120 hours at 37°C in a CO_2 incubator. For cytotoxicity assay under 3D cell culture condition, cells were seeded in a 96-well U bottom ultra-low binding plates for 3 days to allow spheroid formation and treated with a serial dilution of ADC for 10 days at 37°C in a CO_2 incubator. For cell viability measurement, CellTiter-Glo reagent (Promega) or 3D Titer-Glo reagent (Promega) was added into each well at equal volume. Relative luminescence was measured on an ENVISION plate reader (Perkin-Elmer) and converted to % viability using untreated cells as controls. Data was analyzed by GraphPad Prism using nonlinear regression analysis, log (inhibitor) versus response, variable slope, 4-parameter fit equation.

Tubulin polymerization assay

Porcine MAP-rich tubulin (Cytoskeleton Inc.) was dissolved in cold GPME buffer (80 mmol/L Na-PIPES, pH 6.9, 1 mmol/L MgCl2, and 0.5 mmol/L EGTA with 1 mmol/L GTP) at 2.5 mg/mL final concentration. 10 μL of the testing drugs diluted in GPEM buffer or DMSO control (0.02% DMSO diluted in GPEM buffer) were dispensed into each well of a transparent 96-well half area flat bottom plate. 100 μL of the prepared Porcine MAP-rich tubulin was rapidly added into each well of the plate. Absorbance at 340 nm was measured every minute after adding the tubulin buffer for 60 minutes at 37°C on a SpectraMax M5 (Molecular Devices). Data were plotted as absorbance at 340 nm versus time in minutes using GraphPad Prism.

Evaluation of *in vitro* and *in vivo* stability of STRO-002

For *in vitro* stability study, STRO-002 was incubated with human or cynomolgus monkey plasma (Bioreclamation) or PBS at a final concentration of 100 μg/mL at 37°C in a CO_2 incubator for up to 21 days. For *in vivo* stability, non-tumor bearing (for PK study) or Igrov1 bearing (for *in vivo* SC209 release study) female SCID Beige mice [Charles River Laboratories (CRL)] of 8 to 10 weeks of age were dosed with a single intravenous bolus of 5 mg/kg STRO-002. Blood samples ($n = 3$ per time point) were collected at different timepoint for up to 21 days and processed for plasma.

STRO-002 concentration in plasma was determined by quantitative ELISA assays. For *in vitro* stability study, recombinant human FolRα ECD (R&D System) was coated on Nunc MaxiSorp plates. For PK analysis, goat anti-human Fcγ (Jackson ImmunoResearch) was coated. Serial dilutions of samples and standard (purified STRO-002) were added to the ELISA plates and incubated for 1 hour at room temperature. Horseradish peroxidase (HRP)-conjugated goat anti-human IgG (Jackson ImmunoResearch) was then added as detection antibody and incubated for another hour at room temperature. SureBlue Reserve TMB Peroxidase Substrate (KPL Inc) was used for detection and absorbance at 450 nm was measured on a SpectraMax M5 plate reader (Molecular Devices).

To determine the DAR, STRO-002 in plasma samples were captured using Streptavidin Mag Sepharose Beads (GE Healthcare) coated with biotinylated FolRα ECD in HBS-E buffer (0.01 mol/L HEPES pH 7.4, 0.15 mol/L NaCl, 3 mmol/L EDTA). Captured STRO-002 was released from the beads with gentle mixing in 25 μL of 1% formic acid at room temperature for 5 minutes and neutralized with 15 μL 1 mol/L Tris-HCl (pH 9.0). The 40 μL eluted sample was injected into an Agilent 1200 series LC/MS system to measure the DAR.

STRO-002–mediated bystander killing of cells

FolRα-negative Daudi cells were labelled with Oregon Green cell tracer (Thermo Fisher) and cocultured with FolRα-positive Igrov1 cells or A549 at 1:1 ratio in 24-well plates (2×10^5 cells per well). Mixed cells were then treated with serial dilutions of tested in triplicates. After 3 days of treatment, the Daudi cells in the cell culture medium were taken out, stained with fixable viability far-red dyes (Thermo Scientific) and counted on flow cytometer. The bystander effect of STRO-002 was reported as % of live Daudi cells compared with untreated controls versus concentration of STRO-002 in nmol/L. Igrov1, A549 and Daudi cells cultured alone were also treated with STRO-002 as controls.

Cell line–derived xenograft models

All *in vivo* procedures were conducted in compliance with the guidelines of the Institutional Animal Care and Use Committee at Sutro Biopharma or commissioned contract research organization (CRO). Cell line–derived xenograft studies were conducted with the following human ovarian tumor models in the indicated mouse strains: Igrov1 in SCID Beige mice (CRL, Hollister, CA), OVCAR-3 in BALB/c nude mice (study performed at Crown Bioscience CRO), OV-90 in SCID mice (study performed at CRL CRO). In all studies, female animals at 6 to 12 weeks of age were anesthetized with isoflurane and implanted subcutaneously into the right hind flank with 7.5×10^6 Igrov1 cells, 1×10^7 OVCAR3 cells with 1:1 matrigel, or 1×10^7 OV90 cells. Randomization and start of treatment were initiated when the average tumor size was established (100–150 mm^3) or advanced ($\sim$ 400 mm^3) for OVCAR3 tumors and designated Day 0 posttreatment. Animals (n = 7–10 per group) received a single intravenous bolus of the test articles at the indicated dose and dosing schedule in the figures. Body weight and tumor size were monitored twice per week. Tumor volumes were calculated using the formula $(L \times W^2)/2$; where length (L) and width (W) are the longer and shorter values, respectively. The primary study endpoint was designated as the day when the mean of the vehicle control group was at least >1,000 mm^3. Tumor growth inhibition (TGI) is determined on the day the vehicle group reaches the primary study endpoint. TGI is calculated as a percentage using the formula $[1-\{(T_{final}-T_{initial})/(C_{final}-C_{initial})\}]^*100$, where T is treatment, C is the mean of vehicle control tumors, and initial size is the tumor size on the first day of treatment. TGI > 100% indicates tumor regression below the starting tumor size. TGI was analyzed using a one-way ANOVA test with the Dunnett multiple comparison test to compare versus vehicle control or Sidaks multiple comparisons test to compare select groups in combination studies. A P value of less than 5% ($P < 0.05$) was considered significant. All data are presented as mean ± SEM. *, $P < 0.05$; **, $P < 0.01$; ***, $P < 0.001$; ***, $P < 0.0001$.

IHC detection of FolRα in patient-derived xenograft models

Formalin-fixed, paraffin-embedded tumor microarrays of human endometrial/uterine patient-derived xenograft (PDX) models were procured from South Texas Accelerated Research Therapeutics

(START) CRO. IHC analysis was performed at Ensigna CRO. Biotinylated anti-FolRα mouse monoclonal antibody (SP9530, Clone, #26B3.F2) was used at 10 μg/mL with citrate-based pH 6.2 Heat-Induced Epitope Retrieval (Biocare, catalog no. DV2004); a diluent only control was used under the same conditions. The sections were blocked with Biocare Peroxidase Blocker (Biocare, catalog no. IPB5000/PX968) and Background Punisher (Biocare, catalog no. BP974), while Avidin and Biotin blockers (Biocare, catalog no. AB972) were used to block endogenous biotin. One-step 4plus Streptavidin HRP-Polymer detection system (Biocare, catalog no. HP604) was used for detection, followed by IntelliPATH FLX DAB chromogen kit (Biocare, catalog no. IPK5010), IntelliPATH Hematoxylin (Biocare, catalog no. IPCS5006) and Ventana Bluing Reagent (Ventana, catalog no. 760–2037) for chromogenic detection and counterstaining.

Endometrial PDX models

Endometrial PDX studies were performed at START CRO. For each PDX model, 1 to 2 mm^3 of tumor fragments (passages 4–8) were implanted subcutaneously into the flank of 6- to 12-week-old female athymic nude mice (Jackson Labs). Due to different PDX tumor growth rates, study enrollment for each model was staggered. Start of treatment was initiated when the average tumor size was approximately 100 to 200 mm^3 (designated as Day 0 posttreatment). Animals ($n = 3$ per group) were randomized and assigned to an untreated control group or 10 mg/kg STRO-002 intravenous treated group administered weekly. Body weight and tumor size were monitored twice per week. The study endpoint was reached when the mean of the vehicle control group was >1,000 mm^3 or until day 45 posttreatment. A complete response was defined as the absence of measurable tumors (0 mm^3) for at least two consecutive measurements. Statistical analysis of TGI was performed using an unpaired *t* test for each PDX model. A *P* value of less than 5% ($P < 0.05$) was considered significant. *, $P < 0.05$; **, $P < 0.01$; ***, $P < 0.001$; ***, $P < 0.0001$.

Data availability

Raw data for this study were generated at Sutro Biopharma and are available within the article and its Supplementary Data files. Derived data supporting the findings of this study are available from the corresponding author upon request.

Results

STRO-002 is a homogeneous anti-FolRα ADC

We have developed a homogeneous FolRα targeting ADC, STRO-002, for the treatment of ovarian and endometrial cancers. STRO-002 consists of a high affinity anti-FolRα antibody (SP8166) covalently conjugated to a novel cleavable 3-aminophenyl hemiasterlin linker-warhead (SC239) with a DAR of 4 (**Fig. 1A**).

The anti-FolRα antibody SP8166 was discovered using ribosome display technology from a synthetic human Fab antibody library previously described (15). Sutro's XpressCF protein expression platform allowed rapid selection of anti-FolRα lead antibodies based on binding affinity, internalization activity, and thermostability. The final anti-FolRα lead antibody (SP8166) showed high affinity binding to human FolRα by SPR ($K_D = 2.3$ nmol/L, **Fig. 1B**). In FACS based cell binding assay, SP8166 binds to human FolRα overexpressed on 293T cells (**Fig. 1C**) or cyno-FolRα overexpressed on CHO-cells (**Fig. 1D**) with similar high affinity while no nonspecific binding to cells that lack FolRα expression. SP8166 binding was specific to FolRα and only showed weak, non-saturating binding to FolRβ, a closely related member of the folate receptor family (**Fig.1C**).

To generate anti-FolRα ADCs, the nonnatural amino acid pAMF was incorporated into the anti-FolRα lead antibodies at specific sites using the *in vitro* protein expression platform XpressCF+. Site-specific conjugation of a linker-payload with a dibenzocyclooctyne (DBCO) moiety was subsequently achieved through the rapid and specific reaction to the pAMF residues using copper-free click chemistry. The specificity and robustness of the XpressCF+ system and conjugation platform enabled rapid make-test cycles to select the best ADC. SC239 is a novel linker-warhead that consists of a 3-aminophenyl hemiasterlin warhead linked to a DBCO moiety through a cathepsin-sensitive val-cit-PABA linker, which can be cleaved in the lysosome to release the free warhead 3-aminophenyl hemiasterlin (SC209; **Fig. 1A**).

To select the best anti-FolRα ADC, multiple anti-FolRα antibodies were conjugated to SC239 at the same conjugation sites at DAR = 4 and tested in cell killing assays as well as *in vivo* mouse TGI efficacy studies (Supplementary Fig. S1A, Supplementary Fig. S2A), two antibodies with best *in vivo* efficacy were picked for further studies. It has been previously shown that variations in conjugation sites led to differences in stability, PK profile as well as *in vivo* efficacy (16). We have explored the *in vitro* and *in vivo* activity of the two lead antibodies conjugated to SC239 at different DARs (Supplementary Fig. S1B) and different sites (Supplementary Fig. S1C, Supplementary Fig. S2B, Supplementary Fig. S2C). ADCs conjugated to another 3-aminophenyl hemiasterlin cleavable linker payload (SC346) were also compared with SC239 ADCs *in vitro* and *in vivo* (Supplementary Fig. S1D and Supplementary Fig. S2D). The anti-FolRα antibody H01 conjugated to SC239 at heavy chain sites Y180 and F404 showed the best *in vitro* properties and *in vivo* efficacy, and later designated as STRO-002. When analyzed by deconvoluted LC-MS/MS, STRO-002 was represented by a single predominant species with a calculated DAR of 3.95 (**Fig. 1E**).

STRO-002 releases a novel 3-aminophenyl hemiasterlin cytotoxic warhead with reduced efflux by P-gP compared with other tubulin inhibitors

Cell surface FolRα can internalize into cells and recycles between endosomal and cell surface compartments (17). To investigate the internalization activity of the anti-FolRα antibody, SP8166 was conjugated to a fluorescent dye (DBCO-Alexa647) and its internalization was tracked in a FACS based assay in FolRα-positive Igrov1 and OVCAR3 cells (Supplementary Table S1). As shown in **Fig. 2A**, fluorescently labeled SP8166 rapidly internalized into cells, with roughly 20% of bound antibody internalizing in the first 30 minutes and 70% internalized by 24 hours (**Fig. 2A**). The internalization of fluorescently labeled SP8166 was also monitored in Igrov1 cells using fluorescent microscopy as shown in **Fig. 2B**. SP8166 was not detected inside the cells at the start of the internalization assay (0 min). After incubation at 37°C, fluorescent signal was detected inside the cells at 30 minutes and increased at 60 minutes.

Upon STRO-002 internalization into FolRα-positive cells, 3-aminophenyl-hemiasterlin (SC209) is released by enzymes in the lysosome as the catabolite. SC209 is a synthetic analogue of hemiasterlin, which is derived from marine sponges and binds to the Vinca-peptide site of tubulin to prevent the polymerization of microtubules (18). In an *in vitro* tubulin polymerization assay, SC209 effectively inhibited tubulin polymerization in a dose dependent manner, similar in potency to another tubulin inhibitor MMAE, but more potent than maytansine at the same concentration (**Fig. 2C**). SC209 and STRO-002 treatment on KB cells induced cell cycle arrest in the G_2–M phase after 24 hrs, leading to increased apoptosis after 48 hours of treatment (Supplementary Fig. S3). In cell proliferation assays, SC209 induced

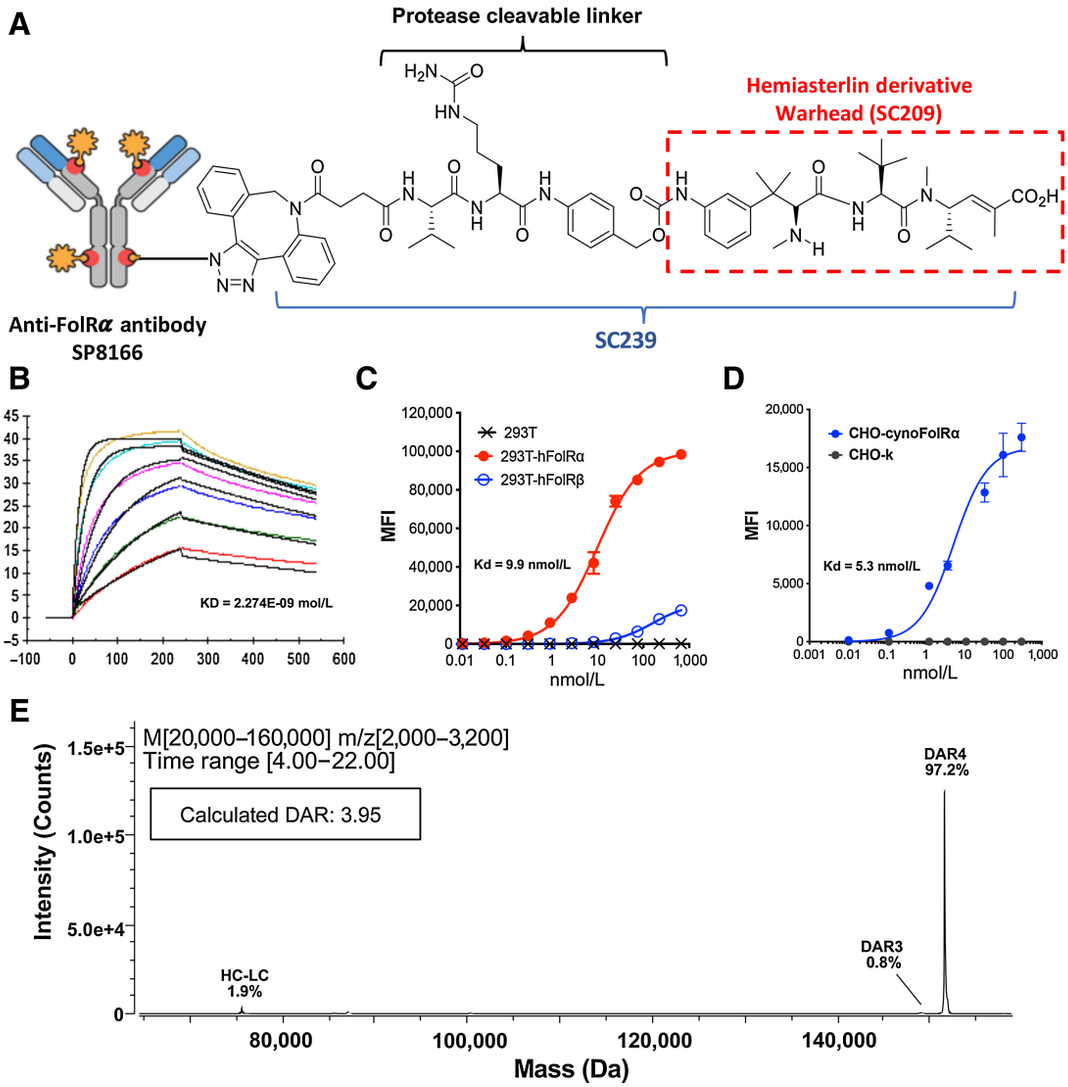

Figure 1.

STRO-002 is a homogeneous anti-FolRα ADC. **A,** The structure of STRO-002, which consists of a high affinity anti-FolRα antibody (SP8166) conjugated to a novel cleavable 3-aminophenyl hemiasterlin linker-warhead (SC239). The released cytotoxic warhead SC209 is indicated in the red box. **B,** The binding kinetics of SP8166 to as determined by SPR shows that the anti-FolRα antibody SP8166 binds to the human FolRα ECD with high affinity. **C,** SP8166 binds with high affinity to human FolRα overexpressed on 293T cells. Only week binding was observed to highly related human FolRβ expressed on 293T cells, while no binding on 293T cells. **D,** SP8166 binds to cynomolgus monkey FolRα overexpressed on CHO cells, while no binding observed on CHO- parental cells. **E,** Deconvoluted LC-MS chromatogram of intact STRO-002, indicating a single dominant peak with calculated DAR of 3.95.

potent cytotoxicity across multiple cell lines from different malignancies with EC_{50} values ranging from 0.2 to 9.2 nmol/L (**Table 1**). On FolRα-positive Igrov1 and KB cells, STRO-002 induced more than 10-fold greater cytotoxicity than SC209 alone, suggesting that specific delivery of SC209 by the anti-FolRα antibody SP8166 results in more efficient cell killing than the warhead alone (**Fig. 2D**). Unconjugated linker-warhead SC239 showed much reduced cell killing activity compared with SC209.

P-glycoprotein 1 (P-gp), also known as multidrug resistance protein 1 (MDR1), is an ATP-dependent efflux pump believed to play a key role in the development of drug resistance (19, 20). The cytotoxicity of SC209 was evaluated on MES-SA/MX cells that express high levels of P-gp (Supplementary Fig. S4) and the parental MES-SA cells that do not express P-gp. Compared with the parental MES-SA cells, P-gp overexpressing MES-SA/MX cells had modestly reduced sensitivity to SC209 (8-fold EC_{50} shift), suggesting that P-gp mediated drug efflux reduced SC209 cytotoxicity (**Fig. 2E**). In the presence of GF120918, a commonly used inhibitor for P-gp, SC209 cytotoxicity returned to levels found in MES-SA parental cells, indicating the difference observed on these two cell lines is mediated by P-gp. In the same experiment, the cytotoxicity of other known P-gp substrates such as DM4 and MMAE was also evaluated and significant shifts in drug potency was observed in the presence and absence of P-gP, approximately 20-fold for DM4 and

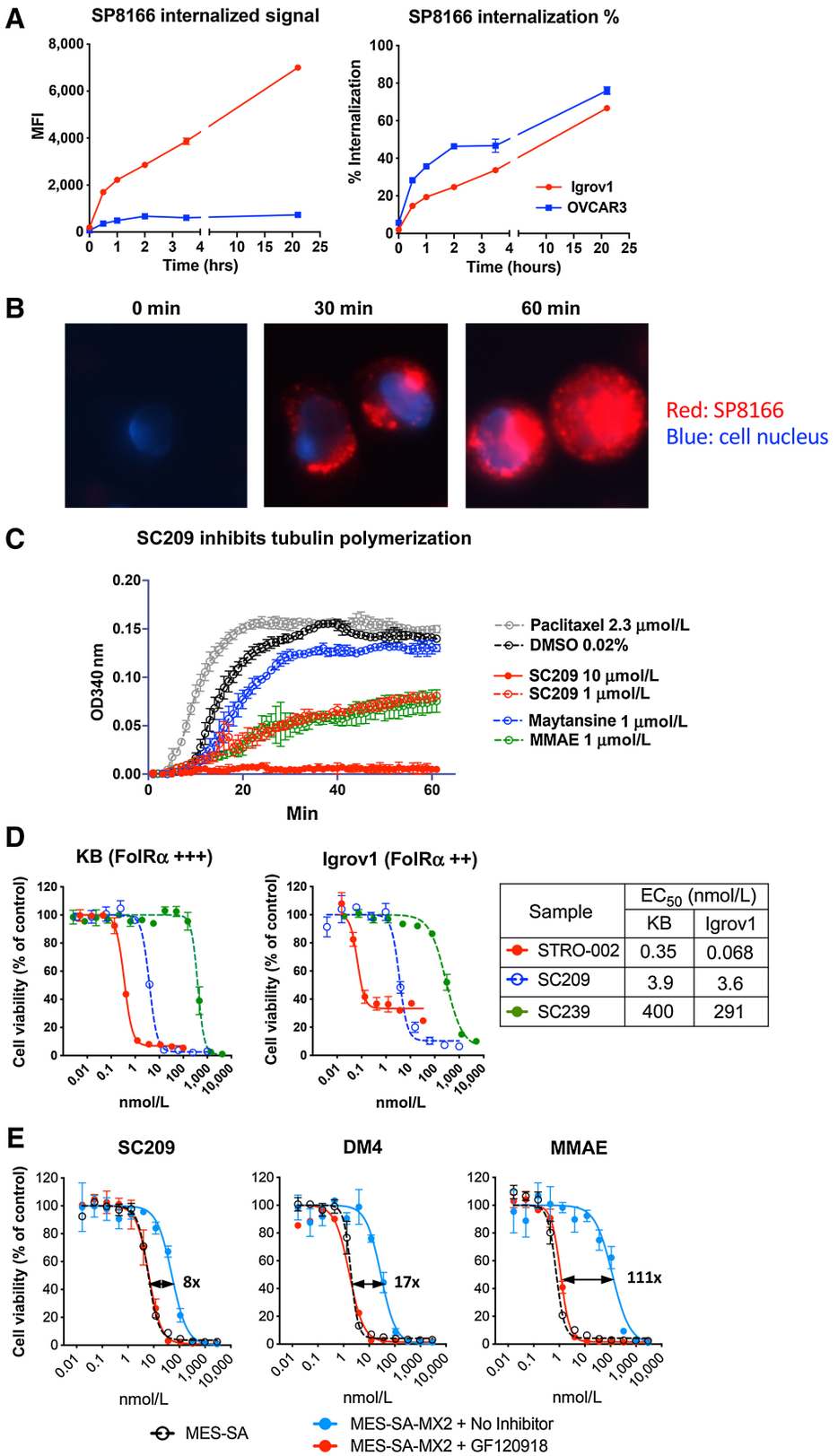

Sample	EC_{50} (nmol/L)	
	KB	Igrov1
STRO-002	0.35	0.068
SC209	3.9	3.6
SC239	400	291

Figure 2.

Characterization of the novel cytotoxin 3-amino-hemiasterlin (SC209) released by STRO-002. **A,** Internalization time course of fluorescently labeled SP8166 into Igrov1 and OVCAR3 cells as determined by FACS-based assay. Total internalized signal is measured by FACS after removing the antibody bound to the cell surface. Percent (%) internalization is the ratio of FACS signal after and before cell surface antibody removal. **B,** Representative fluorescent microscopy images of internalized fluorescently labeled SP8166 in Igrov1 cells. **C,** *In vitro* tubulin polymerization assay shows SC209 is a potent inhibitor of tubulin polymerization, similar to other known tubulin inhibitors (MMAE and Maytansine). **D,** Cytotoxic activity of STRO-002 in target positive Igrov1 cells compared with the free cytotoxin SC209 and the drug-linker SC239. STRO-002 is highly efficient at delivering SC209 into the target positive cells. **E,** SC209-induced cytotoxicity on P-gP expressing MES-SA/MX2 cells in the presence and absence of P-gP inhibitor GF120918, compared with know P-gP substrates DM4 and MMAE. Cell killing EC_{50} fold change with and without GF120918 are indicated on the cell killing curves.

Table 1. SC209 cytotoxicity on different cell lines.

Indications	Cell lines	SC209 cell killing EC_{50}
Ovarian	Igrov1	2.2
	Ishikawa	1.6
	OVKATE	2.8
Breast cancer	SKBR3	1.42
	MDA-MB-453	1.8
	MDA-MB-231	1.7
	MDA-MB-468	0.74
Colon cancer	HCT116	9.18
	HT29	3.18
	Skco1	3.59
Lung cancer	NCI-H1703	0.24
	A549	7.9
	NCI-H1651	9.2
	NCI-H2110	0.84
Skin cancer	MDA-MB-435	2.29
	A431	1.4
Gastric cancer	NCI-N87	2.1
Cervical	KB	2.2
Multiple myeloma	OPM-2	2.42
Lymphoma	SU-DHL-6	1.42

more than 100-fold for MMAE. Our data indicated that SC209 is a relatively weaker P-gp substrate for drug efflux, compared with other commonly used warheads for ADCs, such as DM4 and MMAE, which implies that STRO-002 will be less susceptible to drug resistance mediated by P-gp (**Fig. 2E**).

STRO-002 antibody and drug linkage are stable *in vitro* and *in vivo*

The serum stability of the drug linker has been shown to have a significant impact on the off-target toxicity of an ADC (21). The stability of STRO-002 was evaluated by incubating the ADC in PBS, human, and cynomolgus plasma at 100 μg/mL at 37°C for 3 weeks. At different time points after incubation, the stability of the antibody was estimated by an ELISA specific for anti-FolRα antibodies. Antibody levels in human and cynomolgus monkey plasma were stable over time, similar to antibody levels after incubation in PBS (**Fig. 3A**). To measure the stability of the linker-warhead, STRO-002 in the plasma was captured by beads coated with FolRα ECD, and subject to LC-MS/MS analysis. The relative DAR was calculated using a weighted average of deconvoluted peak areas of DAR0 – DAR4 species. Minimal changes in DAR were observed over 21 days in PBS, human and cynomolgus monkey plasma (**Fig. 3B**). These results suggest that both antibody and linker-warhead portions of STRO-002 are stable in human and cynomolgus monkey plasma.

The *in vivo* stability of STRO-002 was evaluated in non-tumor bearing SCID Beige mice with a single intravenous dose at 5 mg/kg. The total plasma concentration of STRO-002 antibody was measured over time by a quantitative ELISA specific for human Fc. The pharmacokinetic profile of STRO-002 antibody is similar to other reported antibodies with $T_{1/2} = 6.4$ days and clearance rate of 9.6 mL/day/kg (**Fig. 3C**). The linker warhead stability of STRO-002 was evaluated by affinity pull-down of STRO-002 from the mice plasma followed by LC-MS/MS analysis to determine the DAR. As shown in **Fig. 3D**, STRO-002 drug linkages remained intact in blood circulation with the DAR of STRO-002 remained at 3.9 over 21 days.

When a single 5 mg/kg dose of STRO-002 was injected into Igrov1 tumor bearing SCID mice, SC209 was detected predominantly in the tumor environment, but could not be detected in the plasma (**Fig. 3E**, LLOQ = 0.02 ng/mL), which confirmed the tumor specific release of SC209. This data suggests that STRO-002 may afford potent efficacy with limited systemic toxicity in treating patients with FolRα-positive tumors.

STRO-002 induces potent specific cell killing on FolRα-positive cells and bystander cell killing on FolRα-negative cells

In cell-based proliferation assays, STRO-002 induces potent cell killing activity on FolRα-positive Igrov1 and OVSAHO cells, while no cell killing on FolRα-negative A549 was observed (**Fig. 4A**). Furthermore, neither an anti-GFP control ADC with the same DAR4 construction as STRO-002 nor the unconjugated antibody SP8166 affected the viability of Igrov1 cells. In addition, STRO-002 cell killing was inhibited by the presence of 500 nmol/L unconjugated anti-FolRα antibody SP8166 (**Fig. 4A**). These results confirm that the cytotoxicity of STRO-002 is dependent on specific binding of the ADC to FolRα on the tumor cell surface.

Bystander cell killing of target negative cells is an important mechanism of action for ADCs targeting tumor antigens that have heterogeneous expression on tumors (22). In a FACS-based cell viability assay, we demonstrated that STRO-002 was not cytotoxic to FolRα-negative Daudi cells, but bystander cell killing was observed when Daudi cells were cocultured with FolRα-positive Igrov1 cells (**Fig. 4B**). Bystander cell killing activity of STRO-002 was dependent on the presence of FolRα-positive cells in the cell culture system, because Daudi cell killing was not observed when cocultured with FolRα-negative A549 cells. Our results indicated that bystander cell killing could provide an additional mechanism by which STRO-002 controls tumor growth.

The ECD of FolRα is known to be shed from the cell surface and has been detected in the serum of normal and cancer patients (23). Circulating FolRα ECD levels in plasma from healthy individuals and from patients with ovarian and endometrial cancers was measured by ELISA. Shed FolRα was detected at levels up to 1.39 ng/mL and 2.33 ng/mL in normal and endometrial cancer patient serum, respectively, but could be detected up to 80.46 ng/mL in serum from patients with ovarian cancer (**Fig. 4C**). To investigate the impact of shed FolRα on the activity of STRO-002, the cytotoxicity of STRO-002 against FolRα-positive cell lines (Igrov1 and OVCAR3) was measured in the presence of FolRα ECD at relevant concentrations where shed FolRα was observed in patient serum samples (10, 30, and 100 ng/mL). At all concentrations tested, FolRα ECD had little to no impact on the cytotoxicity of STRO-002 *in vitro* against OVCAR3 and Igrov1 cells (**Fig. 4C**), suggesting that shed FolRα circulating in patient serum would have minimal effects on the cytotoxicity of STRO-002 on FolRα-positive tumor cells.

STRO-002 is significantly efficacious as monotherapy or in combination with SOC agents in ovarian tumor models

Evaluation of STRO-002 *in vivo* activity was conducted in three human ovarian adenocarcinoma models, Igrov1, OVCAR3, and OV90, with FolRα expression levels that are comparable with those of biopsies from patients with ovarian cancer (Supplementary Fig. S5). Treatment of established (~150 mm^3) Igrov1 tumors with a single dose of STRO-002 at 10 mg/kg demonstrated potent (107% TGI indicating tumor regression) and target dependent efficacy as evidenced by lack of activity with an unconjugated FolRα antibody or an anti-GFP control ADC conjugated to SC239 (**Fig. 5A**). STRO-

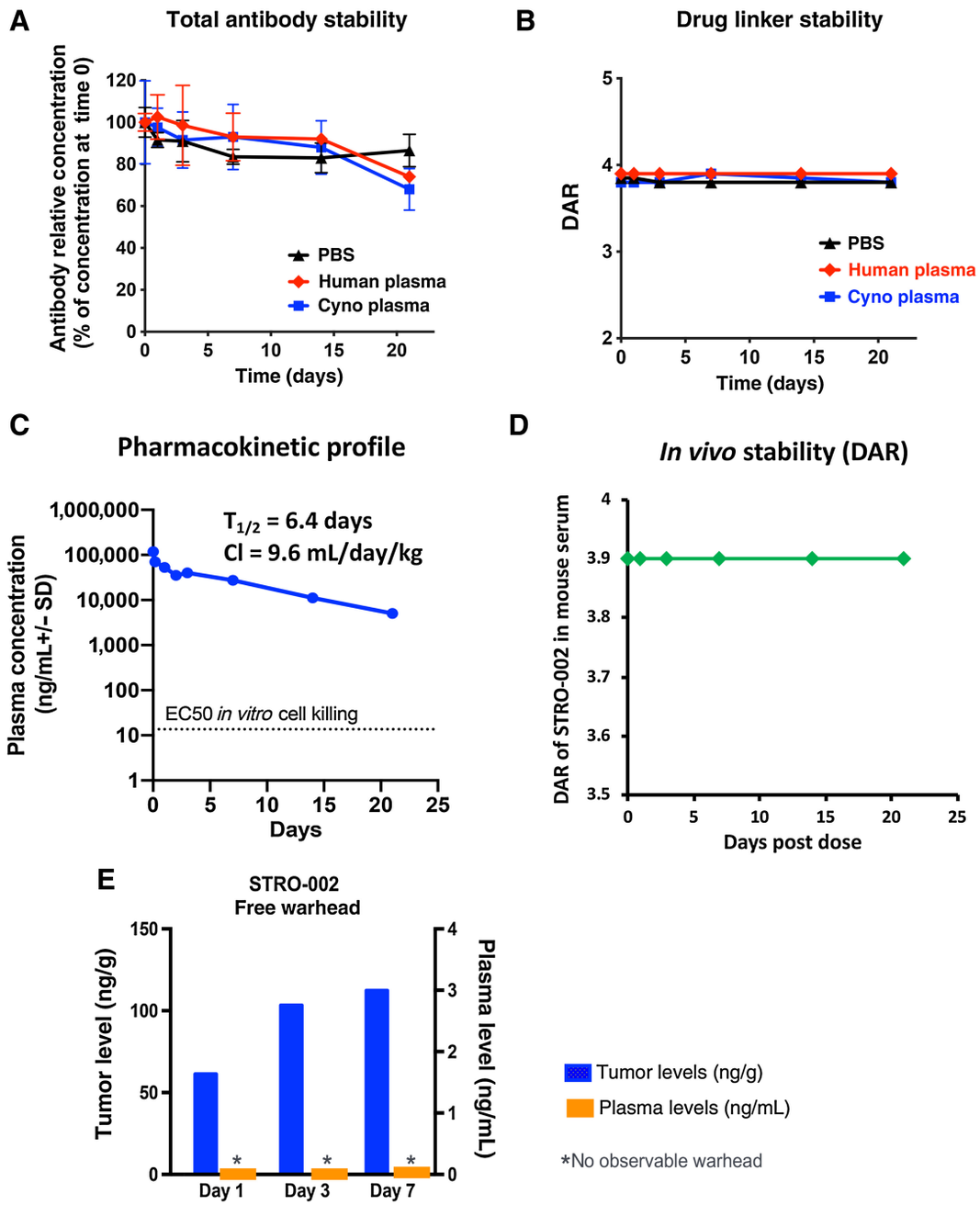

Figure 3.

In vitro and *in vivo* stability of STRO-002. **A,** STRO-002 antibody stability in human plasma and cyno plasma measured by anti-FolRα ELISA shows STRO-002 antibody is stable up to 21 days in plasma. **B,** Drug linker stability of STRO-002 in human and cyno plasma measured by LC/MS demonstrates STRO-002 DAR is stable up to 21 days in plasma. **C,** PK profile of STRO-002 total antibody in non–tumor-bearing mice. STRO-002 displayed PK profile similar to other antibodies. **D,** STRO-002 drug linker is stable for up to 21 days in mice indicated as DAR determined by LC/MS. **E,** Release of SC209 in Igrov1 tumors bearing mice dosed with a single intravenous bolus dose of 5 mg/kg STRO-002. SC209 is only detected in tumor, and not in plasma (LLOQ, 0.02 ng/mL).

002 dose-dependent tumor suppression was established in Igrov1 tumors with significant growth inhibition (68% TGI) starting at a single dose of 2.5 mg/kg (**Fig 5B**). Tumor stasis until day 26 posttreatment was achieved with 5 mg/kg STRO-002, and the highest dose tested (15 mg/kg) induced tumor regression accompanied by sustained growth suppression for >50 days (**Fig. 5B**). Similar dose-dependence and effective growth inhibition was observed in OVCAR3 tumors which express 10-fold lower FolRα compared with Igrov1 (Supplementary Table S1). A single dose of 2.5 mg/kg and 5 mg/kg STRO-002 resulted in 44% and 81% TGI,

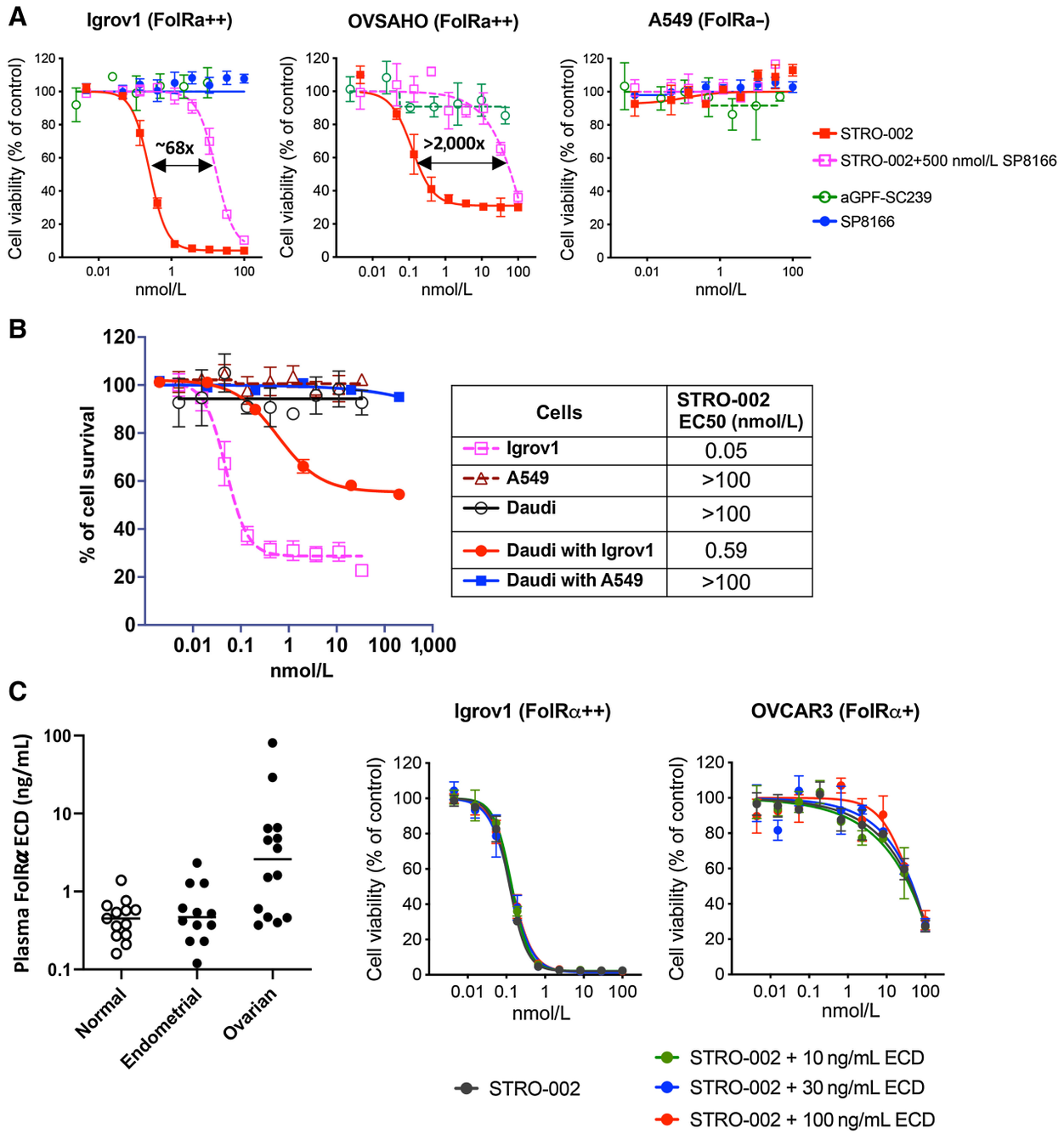

Figure 4.

Specific cell killing activity of STRO-002 on FolRα-positive cells and bystander cell killing activity on FolRα-negative cells. **A,** STRO-002 showed potent cell killing activity in FolRα-positive Igrov1 and OVSAHO cells, while no killing was observed in FolRα-negative A549 cells. The specific killing of Igrov1 and OVSAHO cells can be competed off by adding unconjugated anti-FolRα antibody SP8166. **B,** Bystander killing of FolRα-negative Daudi cells observed when cocultured with target positive Igrov1 cells, but no killing observed when cocultured with FolRα-negative A549 cells. **C,** FolRα ECD concentration in the patient serum samples was detected by ELISA. STRO-002 cytotoxicity was not affected by FolRα ECD at concentrations higher than what have been detected in patient blood samples.

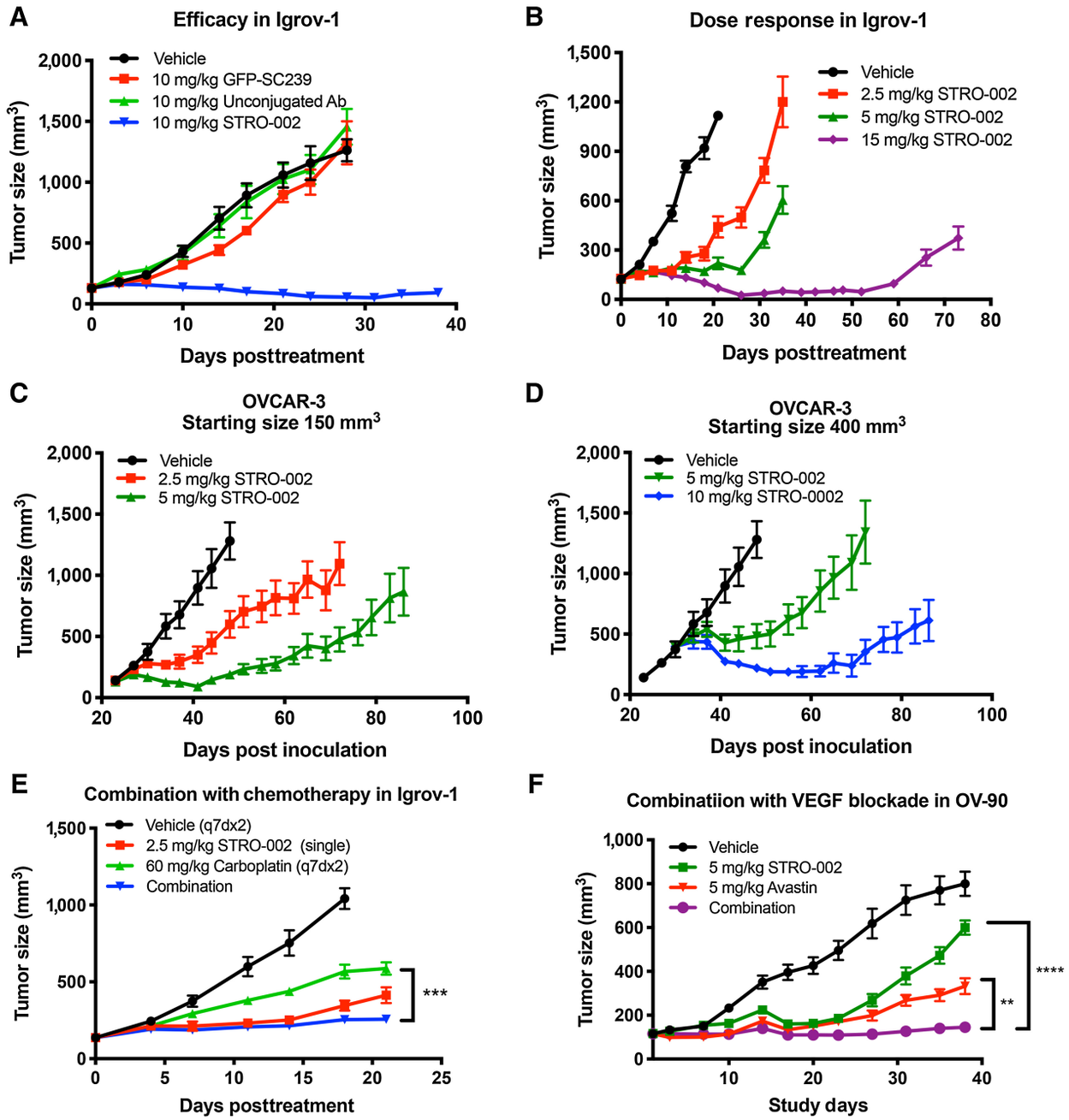

Figure 5.

In vivo efficacy of STRO-002 as monotherapy and in combined with approved SOC therapies in ovarian models. In all studies, treatment was initiated in established tumors [~100–150 mm^3 with a single dose of STRO-002 or specified test article at the indicated dose unless otherwise noted. **A,** Single dose of 10 mg/kg STRO-002 induced tumor regression in Igrov1 tumors. Equivalent doses of control test articles had no activity. **B,** Dose-dependent STRO-002 efficacy is observed in Igrov1 tumors starting at 2.5 mg/kg. **C** and **D,** OVCAR3 tumors showed similar dose responsiveness to STRO-002 in established (**C**) and advanced [400 mm^3 (**D**) tumors. STRO-002 combination treatment with carboplatin (**E**) or anti-VEGF antibody Avastin (**F**) improved efficacy in Igrov1 and OV90 tumors, respectively.

respectively, in established (150 mm^3) OVCAR3 tumors (**Fig. 5C**), while in advanced (~400 mm^3) OVCAR3 tumors, slightly higher doses at 5 and 10 mg/kg elicited comparable TGI at 54% and 86%, respectively (**Fig. 5D**). At the highest dose 10 mg/kg STRO-002 induced OVCAR3 tumor regression without regrowth for up to 60 days post dose (**Fig. 5D**).

Furthermore, STRO-002 combined with approved SOC agents for ovarian cancer patients demonstrated added benefit. Coadministration of a single dose of 2.5 mg/kg STRO-002 with 60 mg/kg carboplatin (q7dx2) resulted in significantly smaller Igrov1 tumors (87% TGI) compared with carboplatin alone (51% TGI; $P = 0.0003$; **Fig. 5E**). In another ovarian model, OV90, the

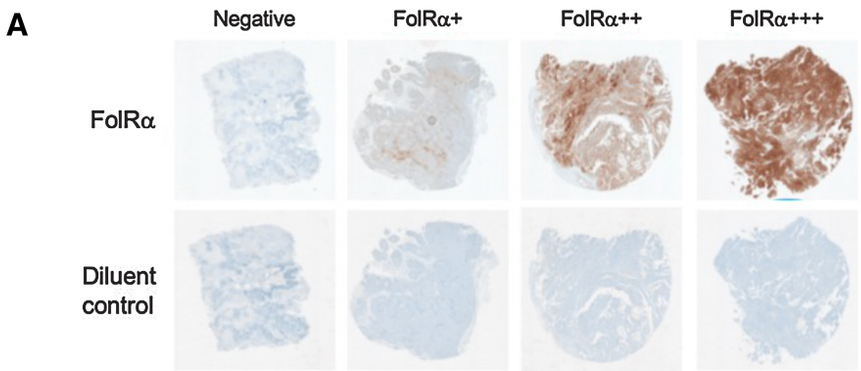

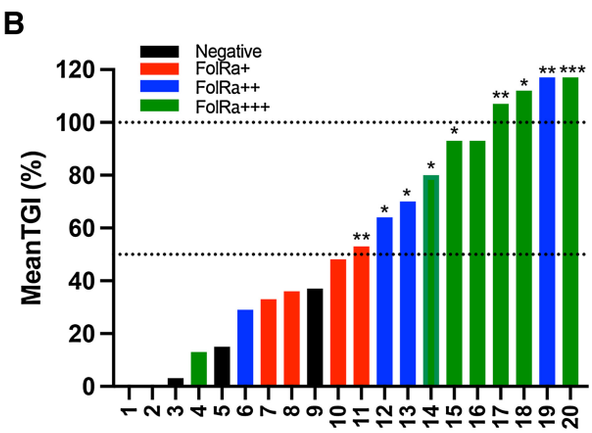

C

FolRα expression	Significant % TGI	Incidence of response
Negative	0/3	0%
FolRα +	1/4	25%
FolRα ++	3/6	50%
FolRα +++	5/7	71%
Total FolRα Positive	**9/17**	**53%**

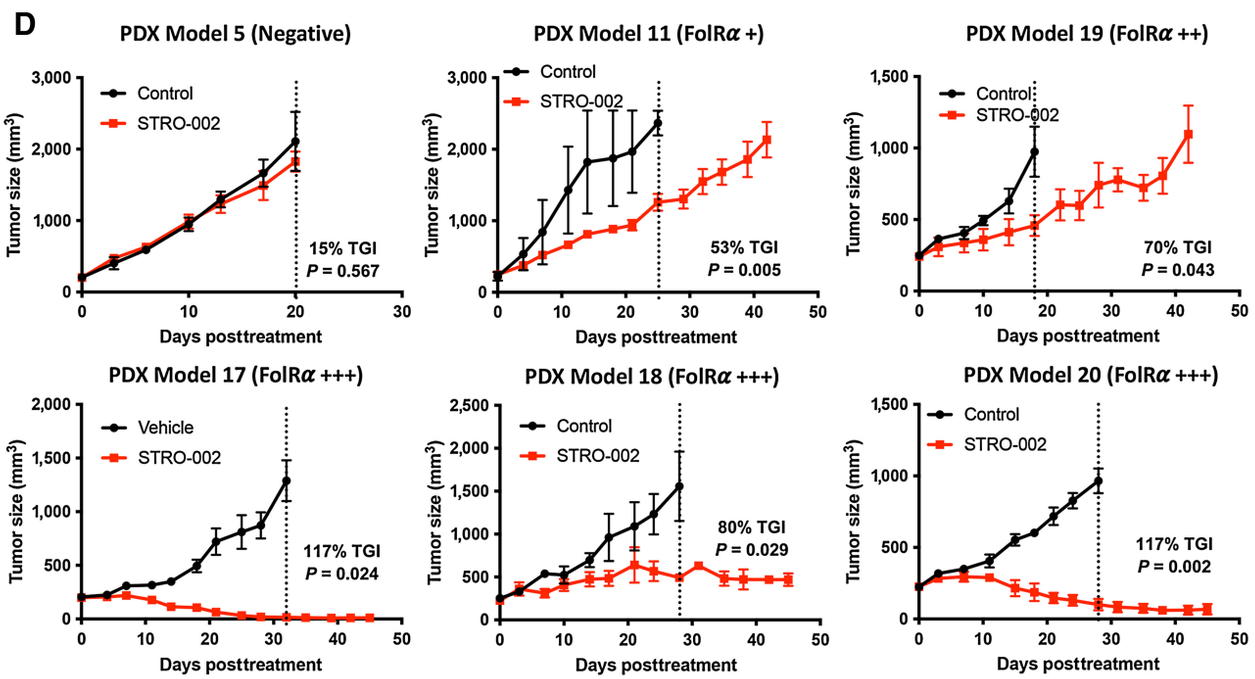

Figure 6.

Robust STRO-002 monotherapy efficacy in endometrial PDX models with different levels of FolRα expression. **A,** Representative IHC images of FolRα expression in endometrial PDX models. **B,** Bar graph shows mean TGI for 20 endometrial PDX tumors in response to weekly 10 mg/kg STRO-002 treatment. Models are color coded based on FolRα expression levels and lines indicate 50% and 100% TGI. **C,** Table summarizes the number of models with statistically significant TGI and incidence of response for PDX models grouped by expression level. **D,** Representative tumor growth curves of endometrial PDX models that express negative, low, moderate, and high FolRα with significant efficacy in response to STRO-002 treatment.

combination of a single dose each of 5 mg/kg STRO-002 plus 5 mg/kg Avastin significantly improved the TGI to 96% versus STRO-002 (29% TGI, $P < 0.0001$) or Avastin (68% TGI, $P < 0.0054$) alone (**Fig. 5F**).

STRO-002 demonstrated significant activity in endometrial PDX models with a range of FolRα expression

The *in vivo* activity of STRO-002 was also assessed in endometrial carcinomas in which FolRα is expressed at lower intensity and frequency compared with ovarian tumors (Supplementary Table S2). Twenty endometrial PDX models with FolRα levels ranging from negative, weak (FolRα+), moderate (FolRα++), and high (FolRα+++) were selected, to correlate expression with response to STRO-002 treatment. **Fig. 6A** shows representative images of PDX tumors with different levels of FolRα expression (top row). The IHC staining was specific to the anti-FolRα antibody, given the absence of staining with the diluent control (bottom row). Results demonstrated that weekly treatment with 10 mg/kg STRO-002 led to significant antitumor activity in 9 out of 17 (53%) FolRα-positive models (**Fig. 6B** and **C**). Statistically significant ($P < 0.05$) efficacy was observed starting at 53% TGI compared with control group (**Fig. 5B**). In four models with high (FolRα+++) and moderate (FolRα++) expression, treatment with STRO-002 induced tumor regression and achieved complete responses with no palpable tumors (as indicated by TGI >100%; **Fig. 6D**). One additional model with high FolRα expression (PDX Model #16) exhibited 93% TGI and also induced tumor regression, but was not statistically significant likely due to tumor growth variability in the control treated animals. A positive correlation was observed between STRO-002 response and FolRα levels with the greatest incidence of significant responders (71%) in the FolRα+++ models (**Fig. 6C**). It is notable that some models with moderate FolRα++ (50%) and weak FolRα+ (25%) expression also exhibited significant activity (**Fig. 6C** and **D**). STRO-002 did not elicit meaningful activity in PDX tumors without FolRα expression as expected (**Fig. 6B** and **C**).

In summary, STRO-002 exhibited antitumor activity in endometrial carcinomas with FolRα expression ranging from FolRα+ to FolRα+++ with a positive correlation between TGI response and FolRα expression.

Discussion

We report here the discovery of STRO-002, a homogeneous FolRα targeting ADC consisting of a high affinity human anti-FolRα antibody site specifically conjugated to a novel linker payload with a DAR of 4. Rapid empirical evaluation of multiple ADC lead molecules was enabled by XtractCF+ and copper-free click chemistry, which allowed the identification of a potential best in class anti-FolRα ADC based on conjugation sites, linker-warhead stability, and potent *in vitro* and *in vivo* antitumor activity.

Traditional stochastic conjugation methods generate ADCs containing a mixture of heterogeneous molecules with varying DARs and sites of conjugation. These heterogeneous species can display significant differences in binding affinity, stability, and pharmacokinetics and pharmacodynamics profiles, leading to variability in toxicity and efficacy in patients. Sutro's XtractCF+ expression system enables the site-specific incorporation of the nonnatural amino acid pAMF in the antibody. Copper-free click chemistry enabled rapid and specific covalent conjugation, which resulted in the consistent production of a homogeneous ADC product optimized for the delivery of a cytotoxic hemiasterlin payload to FolRα expressing tumors.

The Xpress CF+ platform enables the incorporation of pAMF at previously intractable sites of an IgG1 and at multiple sites in the same polypeptide chain. Previously, we reported the rapid and parallel synthesis of numerous variants to identify the optimal sites for pAMF incorporation in an antibody (16). The sites of pAMF incorporation in STRO-002 were carefully selected on the basis of efficiency of pAMF incorporation, SC239 conjugation efficiency and stability, as well as *in vivo* pharmacokinetic profile and efficacy. The resulting STRO-002 clinical lead maintains a similar pharmacokinetic profile as other approved antibody therapies and demonstrates linker-payload stability in plasma. STRO-002 is linked to a cytotoxic 3-aminophenyl-hemiasterlin payload through a cathepsin-sensitive linker that can be cleaved in the tumor microenvironment or upon internalization into tumor cells, lending a specific delivery and cytotoxic profile in tumor cells. In addition, the stability of the linker-warhead in circulation and fast clearance of released small molecule warhead SC209 are predicted to limit the systemic toxicity induced by the free warhead.

STRO-002 contains a novel 3-aminophenyl hemiasterlin, SC209, which is a potent tubulin polymerization inhibitor. In addition, SC209 is a weaker substrate for the cellular efflux pump P-gp, supporting the use of STRO-002 in cancers with increased P-gp that are refractory to other chemotherapies such as platinum agents, PARP inhibitors or some tubulin inhibitors. The release of SC209 by FolRα-positive tumor cells can induce bystander killing of FolRα-negative tumor cells, further increasing STRO-002 efficacy in tumors with heterogeneous or low expression of FolRα.

STRO-002 demonstrated reproducible and significant therapeutic benefit in multiple FolRα expressing xenograft models. In several ovarian adenocarcinoma models with FolRα expression reminiscent of patient levels, a single dose of STRO-002 demonstrated robust, dose dependent, and target dependent antitumor activity. In addition, our results provide encouraging evidence to support beneficial STRO-002 combination strategies with chemotherapy or VEGF blockade. In endometrial PDX tumors, STRO-002 demonstrated significant activity including in models with FolRα++ (moderate) and FolRα+ (weak) expression.

On the basis of our preclinical findings, we believe the optimized and homogeneous STRO-002 molecule affords potent efficacy in FolRα-positive tumors and minimizes systematic off-target toxicity, providing the potential for increased therapeutic index in the clinic and a best-in-class FolRα ADC. The clinical safety and preliminary activity of STRO-002 is currently being assessed in phase I clinical trials in ovarian and endometrial cancer patients (ClinicalTrials.gov Identifier: NCT03748186 and NCT05200364).

Authors' Disclosures

X. Li reports a patent for WO2018/071597 A1 issued and a patent for WO2019055909A1 issued to Sutro Biopharma. C.L. Abrahams reports a patent for WO2018071597A1 issued to Sutro Biopharma and a patent for WO2019055931A1 issued to Sutro Biopharma. H.T. Stephenson reports a patent for US201662407409P pending. T.H. Heibeck reports a patent for; and STRO-002 is a compound currently under clinical development by my employer, Sutro Biopharma, Inc. As such, Sutro and I each have an interest in successful development of STRO-002. No entity other than Sutro or its investors has a financial interest in STRO-002. With regard to patents, Sutro owns several patent families that are relevant to STRO-002, consistent with its ownership of the program. If it is critical, Sutro can identify potentially relevant patent families, but it's not obvious that such disclosure would assist in understanding the scope of any conflicts. R.L. Stafford reports a patent for US10596270B2 issued, a patent for WO2019055931A1 pending, and a patent for WO2014176327A2 pending; and was employed by Sutro Biopharma and currently owns stock in the company. A.Y. Yam reports a patent for FolR antibodies and ADCs pending to Sutro Biopharma. T. Kline reports other support from SutroBio outside the

submitted work; in addition, T. Kline has a patent for WO 2016123582 A1 pending, a patent for WO 2019055931 pending, and a patent for WO 2019055909 A1 pending. V.I. De Almeida reports a patent for combination therapies with anti-folate receptor antibody conjugates pending and a patent for anti-FolRα antibody conjugates and their uses pending. M. Lupher reports At the time the work was conducted I was an employee of Sutro Biopharma, a pharmaceutical company where the research was performed. K. Bedard reports grants from Sutro Biopharma during the conduct of the study. No disclosures were reported by the other authors.

Authors' Contributions

X. Li: Conceptualization, data curation, formal analysis, supervision, investigation, writing–original draft, writing–review and editing. **S. Zhou:** Data curation, investigation, writing–review and editing. **C.L. Abrahams:** Conceptualization, formal analysis, supervision, investigation, writing–original draft, writing–review and editing. **S. Krimm:** Data curation, investigation. **J. Smith:** Data curation, investigation. **K. Bajjuri:** Conceptualization, data curation, investigation, writing–review and editing. **H.T. Stephenson:** Data curation, investigation. **R. Henningsen:** Data curation, investigation. **J. Hanson:** Data curation, investigation. **T.H. Heibeck:** Data curation, investigation. **D. Calarese:** Data curation, investigation. **C. Tran:** Data curation, investigation. **G. Yin:** Conceptualization, data curation, investigation, writing–review and editing. **R.L. Stafford:** Conceptualization, investigation. **A.Y. Yam:** Conceptualization, data curation, investigation, writing–review and editing. **T. Kline:** Conceptualization, investigation, writing–review and editing. **V.I. De Almeida:** Conceptualization, writing–original draft, writing–review and editing. **A.K. Sato:** Conceptualization, supervision. **M. Lupher:** Supervision, writing–review and editing. **K. Bedard:** Supervision, writing–review and editing. **T.J. Hallam:** Conceptualization, supervision, writing–review and editing.

Acknowledgments

The authors thank Crown Bioscience for conducting the actual study related to OVCAR3 xenograph model and START (now XenoSTART) for conducting the actual study for the PDX models. The authors also thank Abigail Yu and Asa Elmore for their help in generating graphics for this publication.

Note

Supplementary data for this article are available at Molecular Cancer Therapeutics Online (http://mct.aacrjournals.org/).

Received May 6, 2022; revised September 12, 2022; accepted November 18, 2022; published first November 30, 2022.

References

1. Brasseur K, Gévry N, Asselin E. Chemoresistance and targeted therapies in ovarian and endometrial cancers. Oncotarget 2016;8:4008–42.
2. Stewart C, Ralyea C, Lockwood S. Ovarian cancer: an integrated review. Seminars Oncol Nurs 2019;35:151–6.
3. Lu KH, Broaddus RR. Endometrial cancer. New Engl J Med 2020;383:2053–64.
4. Brooks RA, Fleming GF, Lastra RR, Lee NK, Moroney JW, Son CH, et al. Current recommendations and recent progress in endometrial cancer. Ca Cancer J Clin 2019;69:258–79.
5. Ledermann JA, Canevari S, Thigpen T. Targeting the folate receptor: diagnostic and therapeutic approaches to personalize cancer treatments. Ann Oncol 2015; 26:2034–43.
6. Cheung A, Bax HJ, Josephs DH, Ilieva KM, Pellizzari G, Opzoomer J, et al. Targeting folate receptor alpha for cancer treatment. Oncotarget 2016;7: 52553–74.
7. Kalli KR, Oberg AL, Keeney GL, Christianson TJH, Low PS, Knutson KL, et al. Folate receptor alpha as a tumor target in epithelial ovarian cancer. Gynecol Oncol 2008;108:619–26.
8. Peters C, Brown S. Antibody–drug conjugates as novel anticancer chemotherapeutics. Biosci Rep 2015;35:e00225.
9. Fu Z, Li S, Han S, Shi C, Zhang Y. Antibody–drug conjugate: the "biological missile" for targeted cancer therapy. Signal Transduct Target Ther 2022;7:93.
10. Vergote I, Armstrong D, Scambia G, Teneriello M, Sehouli J, Schweizer C, et al. A randomized, double-blind, placebo-controlled, phase iii study to assess efficacy and safety of weekly farletuzumab in combination with carboplatin and taxane in patients with ovarian cancer in first platinum-sensitive relapse. J Clin Oncol 2016;34:2271–8.
11. Moore KN, Oza AM, Colombo N, Oaknin A, Scambia G, Lorusso D, et al. Phase III, randomized trial of mirvetuximab soravtansine versus chemotherapy in patients with platinum-resistant ovarian cancer: primary analysis of FORWARD I. Ann Oncol 2021;32:757–65.
12. Furuuchi K, Rybinski K, Fulmer J, Moriyama T, Drozdowski B, Soto A, et al. Antibody–drug conjugate MORAb-202 exhibits long-lasting antitumor efficacy in TNBC PDx models. Cancer Sci 2021;112:2467–80.
13. Stafford R, Yam A, Li X, Yin G, Kline T, Abrahams C, De Almeida V, inventors. Anti-folate receptor alpha antibody conjugates and their uses. Patent WO2019055931.
14. Zimmerman ES, Heibeck TH, Gill A, Li X, Murray CJ, Madlansacay MR, et al. Production of site-specific antibody–drug conjugates using optimized nonnatural amino acids in a cell-free expression system. Bioconjugate Chem 2014;25: 351–61.
15. Stafford RL, Matsumoto ML, Yin G, Cai Q, Fung JJ, Stephenson H, et al. In vitro Fab display: a cell-free system for IgG discovery. Protein Eng Des Sel 2014;27:97–109.
16. Yin G, Stephenson HT, Yang J, Li X, Armstrong SM, Heibeck TH, et al. RF1 attenuation enables efficient nonnatural amino acid incorporation for production of homogeneous antibody–drug conjugates. Sci Rep 2017;7:3026.
17. Tsai EHR, Bentz BZ, Chelvam V, Gaind V, Webb KJ, Low PS. In vivo mouse fluorescence imaging for folate-targeted delivery and release kinetics. Biomed Opt Express 2014;5:2662–78.
18. Loganzo F, Discafani CM, Annable T, Beyer C, Musto S, Hari M, et al. HTI-286, a synthetic analogue of the tripeptide hemiasterlin, is a potent antimicrotubule agent that circumvents P-glycoprotein–mediated resistance in vitro and in vivo. Cancer Res 2003;63:1838–45.
19. Szakács G, Paterson JK, Ludwig JA, Booth-Genthe C, Gottesman MM. Targeting multidrug resistance in cancer. Nat Rev Drug Discov 2006;5:219–34.
20. Loganzo F, Sung M, Gerber H-P. Mechanisms of resistance to antibody–drug conjugates. Mol Cancer Ther 2016;15:2825–34.
21. Su Z, Xiao D, Xie F, Liu L, Wang Y, Fan S, et al. Antibody–drug conjugates: recent advances in linker chemistry. Acta Pharm Sinica B 2021;11:3889–3907.
22. Li F, Emmerton KK, Jonas M, Zhang X, Miyamoto JB, Setter JR, et al. Intracellular released payload influences potency and bystander-killing effects of antibody–drug conjugates in preclinical models. Cancer Res 2016;76:2710–9.
23. Leung F, Dimitromanolakis A, Kobayashi H, Diamandis EP, Kulasingam V. Folate receptor 1 (FOLR1) protein is elevated in the serum of ovarian cancer patients. Clin Biochem 2013;46:1462–8.